Thermalization of Nonequilibrium Electron-Positron-Photon Plasmas

A. G. Aksenov,* R. Ruffini, and G. V. Vereshchagin
ICRANet, p.le della Repubblica, 10, 65100 Pescara, Italy and ICRA
and Physics Department, University of Rome "Sapienza", p.le A. Moro 5, 00185 Rome, Italy
(Received 3 June 2007; published 20 September 2007)

Starting from a nonequilibrium configuration we analyze the role of the direct and the inverse binary and triple interactions in reaching thermal equilibrium in a homogeneous isotropic pair plasma. We focus on energies in the range 0.1–10 MeV. We numerically integrate the relativistic Boltzmann equation with the exact QED collisional integrals taking into account all binary and triple interactions. We show that first, when a detailed balance is reached for all binary interactions on a time scale $t_k \lesssim 10^{-14}$ sec, photons and electron-positron pairs establish kinetic equilibrium. Subsequently, when triple interactions satisfy the detailed balance on a time scale $t_{\rm eq} \lesssim 10^{-12}$ sec, the plasma reaches thermal equilibrium. It is shown that neglecting the inverse triple interactions prevents reaching thermal equilibrium. Our results obtained in the theoretical physics domain also find application in astrophysics and cosmology.

DOI: 10.1103/PhysRevLett.99.125003 PACS numbers: 52.27.Ep, 05.20.Dd

An electron-positron plasma is of interest in many fields of physics and astrophysics: the early Universe [1], gamma-ray bursts [2], active galactic nuclei [3], the center of our galaxy [4], hypothetical quark stars [5], and ultra-intense lasers [6].

A detailed study of the relevant processes and possible equilibrium configurations in an optically thin pair plasma is given in [7]. In all the above-mentioned applications the precise knowledge of the optically thick plasma evolution is required. In this case there exists only a qualitative description, and an assumption of thermal equilibrium is often adopted without explicit proof [2].

In this Letter we consider a uniform isotropic electron-positron-photon plasma in the absence of external electromagnetic fields and we describe its evolution starting from arbitrary nonequilibrium initial conditions up to reaching thermal equilibrium. We are interested in the range of final temperatures in thermal equilibrium, bracketing the electron rest mass energy

$$0.1 \lesssim T_{\rm th} \lesssim 10 \text{ MeV}. \tag{1}$$

These boundaries are required for the study of electron-positron pairs in the absence of the production of other particles such as muons. We assume that the energy density of the plasma is constant and is, correspondingly, in the range $1.6 \times 10^{22} < \rho < 3.8 \times 10^{30}$ erg/cm^3. The relative number densities at thermal equilibrium will be $3.1 \times 10^{28} < n_{\rm th} < 7.9 \times 10^{34}$ cm^{-3}.

We adopt a kinetic description for the distribution functions of electrons, positrons, and photons. In our case the plasma parameter is small, $g = (nr_D^3)^{-1} \ll 1$, where r_D is the Debye length, and therefore we use one-particle distribution functions. Additionally, in our case electrons and positrons are nondegenerate. We solve numerically the relativistic Boltzmann equations [8] which for homogeneous and isotropic distribution functions of electrons, positrons, and photons reduce to

$$\frac{1}{c}\frac{\partial f_i}{\partial t} = \sum_q (\eta_i^q - \chi_i^q f_i), \tag{2}$$

where $f_i(\varepsilon, t)$ are their distribution functions, the index i denotes the type of particle, ε is their energy, and η_i^q and χ_i^q are the emission and the absorption coefficients for the production of a particle of type "i" via the physical process labeled by q.

In order to solve Eq. (2) we use a finite difference method by introducing a computational grid in the phase space to represent the distribution functions and to compute collisional integrals [9]. The result of this procedure is the stiff system of ordinary differential equations to be solved with the implicit Gear method [10]. For binary interactions we use exact QED matrix elements [11]. For triple interactions we compute emission and absorption coefficients following Svensson [12]. The Compton scattering of photons, for instance, is described by [9]

$$\eta_\gamma^{\rm cs} = \int d\mathbf{k}' d\mathbf{p} d\mathbf{p}' w_{\mathbf{k}'\mathbf{p}';\mathbf{k},\mathbf{p}} f_\gamma(\mathbf{k}', t) f_\pm(\mathbf{p}', t), \tag{3}$$

$$\chi_\gamma^{\rm cs} f_\gamma = \int d\mathbf{k}' d\mathbf{p} d\mathbf{p}' w_{\mathbf{k}'\mathbf{p}';\mathbf{k},\mathbf{p}} f_\gamma(\mathbf{k}, t) f_\pm(\mathbf{p}, t), \tag{4}$$

where

$$w_{\mathbf{k}'\mathbf{p}';\mathbf{k},\mathbf{p}} = \frac{1}{(2\pi\hbar)^2}\delta^4(k + p - k' - p')\frac{|M_{fi}|^2}{16\varepsilon_\gamma \varepsilon_\pm \varepsilon'_\gamma \varepsilon'_\pm} \tag{5}$$

is the corresponding transition probability, $k = (\epsilon_\gamma/c, \mathbf{k})$ and $p = (\epsilon_e/c, \mathbf{p})$ are four-momenta of photon and positron (electron), primes denote particles after the interaction, and M_{fi} is the matrix element for the considered process.

For such a dense plasma collisional integrals in (2) should include not only binary interactions, having order

α in Feynmann diagrams, where α is the fine structure constant, but also triple ones, having order α^2 [11]. We consider all possible binary and triple interactions between electrons, positrons, and photons as summarized in Table I.

Each of the above reactions is characterized by the corresponding time scale and optical depth. For Compton scattering, for instance, we have

$$t_{\rm cs} = \frac{1}{\sigma_T n_\pm c}, \qquad \tau_{\rm cs} = \sigma_T n_\pm R_0, \tag{6}$$

where σ_T is the Thomson cross section and $n_\pm$ is the number density of pairs. There are two time scales in our problem that characterize the condition of detailed balance between direct and inverse reactions, $\sim t_{\rm cs}$ for binary and $\alpha^{-1} t_{\rm cs}$ for triple interactions, respectively. In the first phase of the system evolution the binary interactions are found to have a predominant role. Starting from arbitrary distribution functions we find a common development: at the time $t_{\rm cs}$ the distribution functions always have evolved in a functional form on the entire energy range, depending only on two parameters. We find in fact for the distribution functions the expressions

$$f_i(\varepsilon) = \exp\left(-\frac{\varepsilon - \varphi_i}{\theta_i}\right), \tag{7}$$

with chemical potential $\varphi_i \equiv \mu_i / m_e c^2$ and temperature $\theta_i \equiv k_B T_i / m_e c^2$, where $\varepsilon \equiv \epsilon / m_e c^2$ is the energy of the particle, m_e is the electron mass, and k_B is Boltzmann's constant. Such a configuration corresponds to a kinetic equilibrium [13,14] in which electrons, positrons, and photons acquire a common temperature and nonzero chemical potential. At the same time we found that triple interactions become essential for $t > t_{\rm cs}$, after the establishment of kinetic equilibrium. Such triple interactions, both direct and inverse, are indeed essential in achieving the thermal equilibrium.

In (7) analogously to the temperature, defining the average kinetic energy in the system, the chemical potential represents deviation from the thermal equilibrium through the relation $\varphi = \theta \ln(n/n_{\rm eq})$, where $n_{\rm eq}$ are concentrations of particles in thermal equilibrium. We do not absorb the chemical potentials into the normalization factors since they depend on time and describe the approach to thermal equilibrium.

TABLE I. Microphysical processes in the pair plasma.

Binary interactions	Radiative variants
Møller, Bhabha $e^\pm e^{\pm\prime} \leftrightarrow e^{\pm\prime\prime} e^{\pm\prime\prime\prime}$ $e^\pm e^\mp \leftrightarrow e^{\pm\prime} e^{\mp\prime}$	Bremsstrahlung $e^\pm e^{\pm\prime} \leftrightarrow e^{\pm\prime\prime} e^{\pm\prime\prime\prime} \gamma$ $e^\pm e^\mp \leftrightarrow e^{\pm\prime} e^{\mp\prime} \gamma$
Single Compton $e^\pm \gamma \leftrightarrow e^\pm \gamma'$	Double Compton $e^\pm \gamma \leftrightarrow e^{\pm\prime} \gamma' \gamma''$
Pair production and annihilation $\gamma\gamma' \leftrightarrow e^\pm e^\mp$	Radiative pair production and three photon annihilation $\gamma\gamma' \leftrightarrow e^\pm e^\mp \gamma''$ $e^\pm \gamma \leftrightarrow e^{\pm\prime} e^\mp e^{\pm\prime\prime}$ $e^\pm e^\mp \leftrightarrow \gamma\gamma'\gamma''$

The results of numerical simulations are reported below. We choose two limiting initial conditions with flat spectra: (i) electron-positron pairs with a 10^{-5} energy fraction of photons and (ii) the reverse case, i.e., photons with a 10^{-5} energy fraction of pairs. Our grid consists of 60 energy intervals and 16×32 intervals for two angles characterizing the direction of the particle momenta. In both cases the total energy density is $\rho = 10^{24}$ erg/cm^3. In the first case initial concentration of pairs is 3.1×10^{29} cm^{-3}, in the second case the concentration of photons is 7.2×10^{29} cm^{-3}.

In Fig. 1 we show concentrations of photons and pairs as well as their sum for both our initial conditions. After calculations begin, concentrations and energy density of photons (pairs) increase rapidly with time, due to annihilation (creation) of pairs by the reaction $\gamma\gamma' \leftrightarrow e^\pm e^\mp$. Then, in the kinetic equilibrium phase, concentrations of each component stay almost constant, and the sum of concentrations of photons and pairs remains unchanged. Finally, both individual components and their sum reach stationary values. If one compares and contrasts both cases as reproduced in Fig. 1 one can see that, although the initial

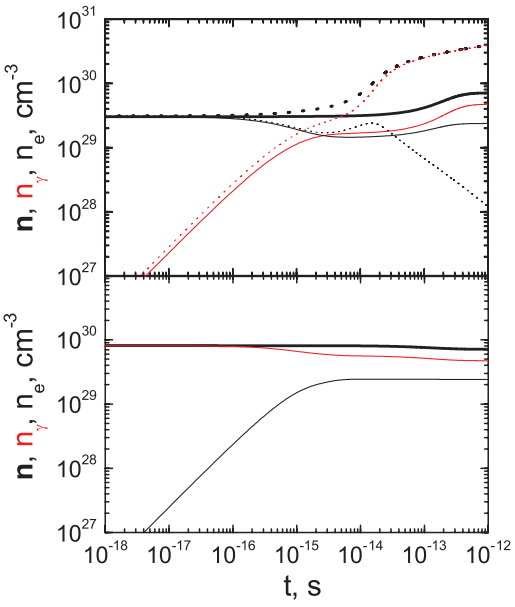

FIG. 1 (color). Dependence on time of concentrations of pairs (black), photons (red), and both (thick line) when all interactions take place (solid line). Upper (lower) figure corresponds to the case when initially there are mainly pairs (photons). Dotted curves on the upper figure show concentrations when inverse triple interactions are neglected. In this case an enhancement of the pairs occurs with the corresponding increase in photon number and thermal equilibrium is never reached.

conditions are drastically different, in both cases the same asymptotic values of the concentration are reached.

We now describe in detail the case when initially pairs dominate. One can see in Fig. 2 that the spectral density of photons and pairs [9]

$$\frac{dE_i}{d\varepsilon} = \frac{4\pi}{c^3} f(\varepsilon, t)\varepsilon^3 \beta_i, \tag{8}$$

where $\beta_\pm = \sqrt{1-(m_e c^2/\varepsilon)^2}$ for pairs and $\beta_\gamma = 1$ for photons, E is the energy density, can be fitted already at $t_k \approx 20 t_{cs} \simeq 7 \times 10^{-15}$ sec by distribution functions (7) with definite values of temperature $\theta_k(t_{cs}) \approx 1.2$ and chemical potential $\varphi_k(t_k) \approx -4.5$, common for pairs and photons. As expected, after t_k the distribution functions preserve their form (7) with the values of temperature and chemical potential changing in time, as shown in Fig. 3. As one can see from Fig. 3, the chemical potential evolves with time and reaches zero at the moment $t_{th} \approx \alpha^{-1} t_k \simeq 710^{-13}$ sec , corresponding to the final stationary solution.

We now discuss the results. Let us consider the distribution functions (7) with different temperatures θ_i and chemical potentials φ_i for pairs and photons. The requirement of vanishing reaction rate for the Compton scattering

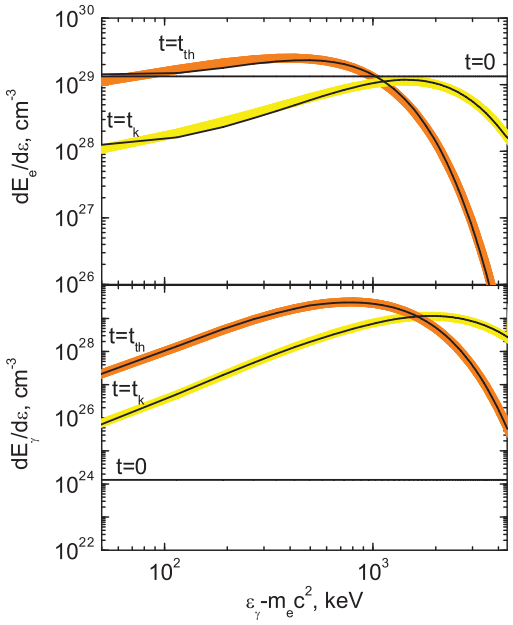

FIG. 2 (color). Spectra of pairs (upper figure) and photons (lower figure) when initially only pairs are present. The black curve represents the results of numerical calculations obtained successively at $t = 0$, $t = t_k$, and $t = t_{th}$ (see the text). Both spectra of photons and pairs are initially taken to be flat. The yellow curves indicate the spectra obtained from (7) at $t = t_k$. The perfect fit of the two curves is most evident in the entire energy range leading to the first determination of the temperature and chemical potential both for pairs and photons. The orange curves indicate the final spectra as thermal equilibrium is reached.

$f_\pm f_\gamma = f'_\pm f'_\gamma$ leads to the equal temperature of pairs and photons $\theta_\pm = \theta_\gamma \equiv \theta_k$; see also [13,14]. In this way the detailed balance between any direct and the corresponding inverse reactions shown in Table I leads to relations between θ and φ collected in Table II.

These relations are not imposed, but are verified through the numerical calculations. This is a powerful tool to verify the consistency of our approach and numerical calculations. These relations were obtained for the first time, to our knowledge, in [14] and then later in [13] for binary reactions.

From Table II one can see that the necessary condition for thermal equilibrium in the pair plasma is detailed balance between direct and inverse triple interactions. This point is usually neglected in the literature where there are claims that the thermal equilibrium may be established with only binary interactions [15]. In order to demonstrate it explicitly we also show in Fig. 1 the dependence of concentrations of pairs and photons when inverse triple interactions are artificially switched off. In this case (see dotted curves in the upper part of Fig. 1), after kinetic equilibrium is reached concentrations of pairs decrease monotonically with time, and thermal equilibrium is never reached.

The existence of a non-null chemical potential for photons indicates the departure of the distribution function from the one corresponding to thermal equilibrium. Negative (positive) value of the chemical potential gener-

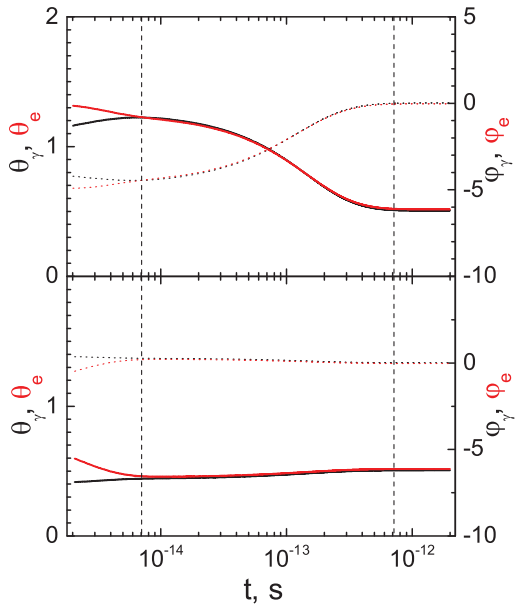

FIG. 3 (color). Time dependence of temperatures, measured on the left axis (solid line), and chemical potentials, measured on the right axis (dotted line), of electrons (black) and photons (red). The dashed lines correspond to the reaching of the kinetic ($\sim 10^{-14}$ sec) and the thermal ($\sim 10^{-12}$ sec) equilibria. Upper (lower) figure corresponds to the case when initially there are mainly pairs (photons).

TABLE II. Relations between parameters of equilibrium DFs fulfilling detailed balance conditions for each of the reactions shown in Table I.

Interaction	Parameters of distribution functions
Compton scattering	$\theta_\gamma = \theta_\pm$, $\forall \varphi_\gamma$, $\varphi_\pm$
Pair production	$\varphi_\gamma = \varphi_\pm$, if $\theta_\gamma = \theta_\pm$
Tripe interactions	φ_γ, $\varphi_\pm = 0$, if $\theta_\gamma = \theta_\pm$

ates an increase (decrease) of the number of particles in order to approach the one corresponding to the thermal equilibrium state. Then, since the total number of particles increases (decreases), the energy is shared between more (less) particles and the temperature decreases (increases); see Fig. 3. Clearly, as thermal equilibrium is approached, the chemical potential of photons is zero.

In our example with the energy density 10^{24} erg/cm^3 the thermal equilibrium is reached at $\sim 7 \times 10^{-13}$ sec with the final temperature $T_{\rm th} = 0.26$ MeV. For a larger energy density the duration of the kinetic equilibrium phase, as well as of the thermalization time scale, is smaller. In our entire temperature range (1) we deal with a nondegenerate plasma.

Our results, obtained for the case of a uniform plasma, can only be adopted for a description of a physical system with dimensions $R_0 \gg 1/n\sigma_T = 4.3 \times 10^{-5}$ cm.

The assumption of the constancy of the energy density is only valid if the dynamical time scale $t_{\rm dyn} = [(1/R) \times (dR/dt)]^{-1}$ of the plasma is much larger than the above time scale $t_{\rm th}$ which is indeed true in all the cases of astrophysical interest.

Since we get thermal equilibrium already on the time scale $t_{\rm th} \lesssim 10^{-12}$ sec, and such a state is independent of the initial distribution functions for electrons, positrons, and photons, the sufficient condition to obtain an isothermal distribution on a causally disconnected spatial scale $R > ct_{\rm th} = 10^{-2}$ cm is the request of constancy of the energy density on such a scale as well as, of course, the invariance of the physical laws.

We have considered the evolution of an initially nonequilibrium optically thick electron-positron-photon plasma up to reaching thermal equilibrium. Starting from arbitrary initial conditions we obtain kinetic equilibrium from first principles, directly solving the relativistic Boltzmann equation with collisional integrals computed from QED matrix elements. We have demonstrated the essential role of direct and inverse triple interactions in reaching thermal equilibrium. Our results can be applied in the theories of the early Universe and of gamma-ray bursts, where thermal equilibrium is postulated at the very early stages. These results can in principle be tested in laboratory experiments in the generation of electron-positron pairs.

We thank the anonymous referee for comments which have improved the comprehension of our results.

*Also at: Institute for Theoretical and Experimental Physics, B. Cheremushkinskaya 25, 117218 Moscow, Russia.

[1] E. W. Kolb and M. S. Turner, *The Early Universe* (Addison-Wesley, Redwood City, CA, 1990).
[2] J. Goodman, Astrophys. J. **308**, L47 (1986); T. Piran, Phys. Rep. **314**, 575 (1999); R. Ruffini *et al.*, Astron. Astrophys. **350**, 334 (1999); Astron. Astrophys. **359**, 855 (2000).
[3] J. F. C. Wardle *et al.*, Nature (London) **395**, 457 (1998).
[4] E. Churazov *et al.*, Mon. Not. R. Astron. Soc. **357**, 1377 (2005).
[5] V. V. Usov, Phys. Rev. Lett. **80**, 230 (1998).
[6] D. B. Blaschke *et al.*, Phys. Rev. Lett. **96**, 140402 (2006).
[7] G. S. Bisnovatyi-Kogan, Y. B. Zel'dovich, and R. A. Syunyaev, Sov. Astron. **15**, 17 (1971); A. P. Lightman, Astrophys. J. **253**, 842 (1982); R. Svensson, Astrophys. J. **258**, 335 (1982); P. W. Guilbert and S. Stepney, Mon. Not. R. Astron. Soc. **212**, 523 (1985); P. S. Coppi and R. D. Blandford, Mon. Not. R. Astron. Soc. **245**, 453 (1990); S. Iwamoto and F. Takahara, Astrophys. J. **601**, 78 (2004).
[8] S. T. Belyaev and G. I. Budker, Dokl. Akad. Nauk SSSR **107**, 807 (1956) [Sov. Phys. Dokl. **1**, 218 (1956)]; D. Mihalas, *Foundations of Radiation Hydrodynamics* (Oxford, New York, 1984).
[9] A. G. Aksenov, M. Milgrom, and V. V. Usov, Astrophys. J. **609**, 363 (2004).
[10] G. Hall and J. M. Watt, *Modern Numerical Methods for Ordinary Differential Equations* (Oxford University Press, Oxford, 1976).
[11] E. M. Lifshitz, L. P. Pitaevskii, and V. B. Berestetskii, *Quantum Electrodynamics* (Elsevier, New York, 1982); W. Greiner and J. Reinhardt, *Quantum Electrodynamics* (Springer, New York, 2003); A. I. Akhiezer and V. B. Berestetskii, *Quantum Electrodynamics* (Nauka, Moscow, 1981).
[12] R. Svensson, Mon. Not. R. Astron. Soc. **209**, 175 (1984).
[13] R. P. Pilla and J. Shaham, Astrophys. J. **486**, 903 (1997).
[14] J. Ehlers, in *Relativity, Astrophysics and Cosmology*, edited by W. Israel (Reidel, Dordrecht, 1973).
[15] S. Stepney, Mon. Not. R. Astron. Soc. **202**, 467 (1983).